Journal of Alloys and Compounds 509 (2011) 6551–6555

Contents lists available at ScienceDirect

Journal of Alloys and Compounds

journal homepage: www.elsevier.com/locate/jallcom

New complex intermetallic in the Al–Rh–Ru alloy system

L. Meshi[a,*], S. Samuha[a], D. Kapush[b], D. Pavlyuchkov[b,c], B. Grushko[d]

[a] Department of Materials Engineering, Ben-Gurion University of the Negev, Beer-Sheva 84105, Israel
[b] I.N. Frantsevich Institute for Problems of Materials Science, 03680 Kyiv 142, Ukraine
[c] Technical University of Freiberg, Institute of Materials Science,09599 Freiberg, Germany
[d] PGI-5, Forschungszentrum Jülich, D-52425 Jülich, Germany

ARTICLE INFO

Article history:
Received 16 January 2011
Received in revised form 16 March 2011
Accepted 17 March 2011
Available online 29 March 2011

Keywords:
Aluminides of transition metals
Electron diffraction
Structure determination

ABSTRACT

A ternary orthorhombic phase (*Pbma*, $a = 2.34$, $b = 1.62$ and $c = 2.00$ nm) was revealed around the $Al_{77}Rh_{15}Ru_8$ composition. It is structurally related to the Al–Rh and Al–Pd ε-phases.

1. Introduction

The interest in aluminum alloys with transition metals (TM) and, particularly, with the elements of the platinum group is due to the formation of complex periodic and quasiperiodic intermetallic phases attractive for both basic and applied research. These binary and ternary phases are usually formed in compositional ranges between 60 and 85 at.% Al (see Ref. [1] and references therein). Among them, the so-called ε_l-phases forming in the Al–Pd(or Rh)–(TM) alloy systems are especially interesting. The regular structures belonging to the ε_l family are orthorhombic with essentially the same a and b lattice parameters, while their c lattice parameters are related as $1:(1+\tau):(2+\tau):(3+\tau):(4+\tau)$ etc., where τ is the golden mean. The index of ε_l is the number l of the strong $(0\,0\,l)$ reflection corresponding to the interplanar spacing of about 0.2 nm. In the known ε-phases $l = 6, 16, 22, 28, 34\ldots$ (see Ref. [1] and references therein). In particular, ε_6 and ε_{16} were revealed close to 75 at.% Al in Al–Rh in Ref. [2].[1]

In the present work we report on the revelation of a new Al–Rh–Ru structure, which is related to the ε_l-phases but exhibits a τ-times larger basic structural element.

2. Experimental

Samples were produced by mixing Al–Rh and Al–Ru alloys used to determine the corresponding binary phase diagrams published in Refs. [2,3]. The ternary sample alloys were melted under an Ar atmosphere in an inductive furnace equipped with a water-cooled copper crucible, thermally annealed under an Ar atmosphere at 1100 °C for up to 144 h and subsequently water quenched.

The samples were studied by powder X-ray diffraction (XRD, Cu $K_{\alpha 1}$ radiation was used), scanning electron microscopy (SEM) and transmission electron microscopy (TEM). The local phase compositions were determined in SEM by energy-dispersive X-ray analysis (EDX) on polished unetched cross sections. Transmission electron microscopy and precession electron diffraction experiments were carried out on a 200 kV JEOL FasTEM-2010 electron microscope equipped with an energy-dispersive X-ray spectrometer (NORAN) and spinning star precession unit (Nanomegas). Precession electron diffraction patterns were taken with a nearly parallel beam in nanodiffraction (NBD) mode with a spot size of 15 nm. The degree of precession was in the range of 18.5–46.6 mrad. Images and diffraction patterns were recorded by a Gatan slow-scan digital camera. The TEM study was performed on powdered materials dispersed on Cu grids with an amorphous carbon film.

3. Results and discussion

The new structure was revealed in a small compositional region around the $Al_{77}Rh_{15}Ru_8$ composition, which is somewhat richer in Ru than the ternary extension of the Al–Rh ε-phase(s). Fig. 1 compares the powder XRD pattern of the new ternary phase, designated E, to those of the binary ε-phases.

In order to determine the unit cell geometry of the new E-phase a series of precession electron diffraction patterns of different orientations with large angular separations was recorded. Then three diffraction zones of highest symmetry were selected so, that each pair of patterns had a common side of the rectangular basis as seen in Fig. 2a–c. It was reasonable to assume that the patterns (a–c)

* Corresponding author. Tel.: +972 86 472576.
E-mail address: louisa@bgu.ac.il (L. Meshi).

[1] In Ref. [2] they were designated O_1 and O_2 but in more recent reports were renamed ε_{16} and ε_6, respectively, in order to fit to the nomenclature used for isostructural Al–Pd–(T M) phases.

0925-8388/$ – see front matter © 2011 Elsevier B.V. All rights reserved.
doi:10.1016/j.jallcom.2011.03.108

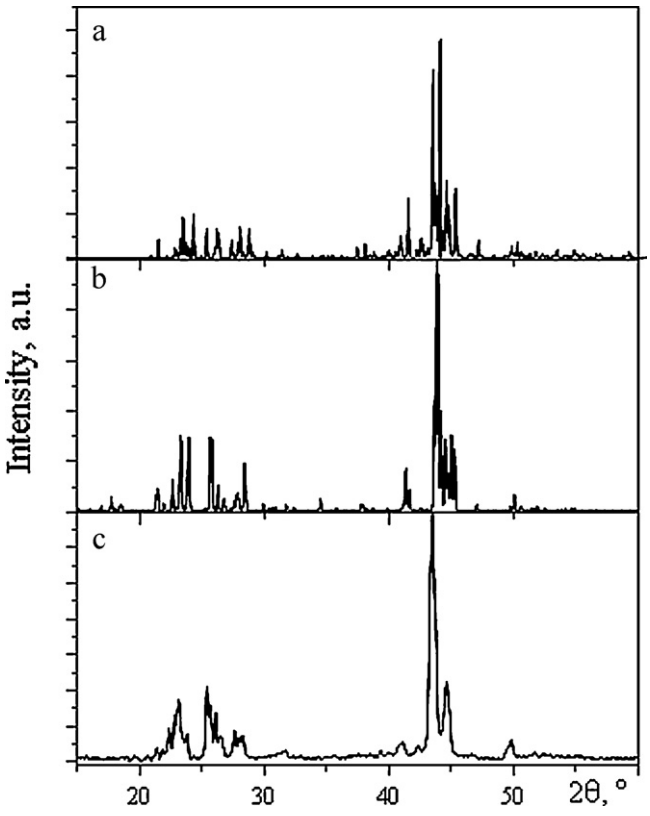

Fig. 1. Powder XRD patterns (Cu $K_{\alpha 1}$ radiation) of the: (a) Al–Rh ε_6-phase, (b) Al–Rh ε_{16}-phase calculated from the data in Ref. [12], and (c) E-phase.

in Fig. 2 could be respectively ascribed to [1 0 0], [0 1 0] and [0 0 1] directions of the orthorhombic crystal lattice, and according to the length of the sides of the rectangular basis the values of the unit cell parameters were estimated as $a = 2.34$, $b = 1.62$ and $c = 2.00$ nm within an accuracy of approximately ±0.004 nm. In terms of this unit cell a successful indexing of all observed diffraction zones was performed thus indicating that the dimensions of the unit cell are correct. The [0 1 0] electron diffraction pattern in Fig. 2b exhibits pseudo-tenfold symmetry, which is typical of the Al–Rh ε-phases (see Ref. [2]). The b lattice parameter of both ε–s and the new structure also corresponds to the periodicity of the decagonal D_4 structure in its specific direction. The decagonal phase of this type (stable or metastable) is observed in several binary and ternary Al–TM alloy systems [1].

Next step in structure determination methodology is evaluation of symmetry of the unit cell. Although convergent beam electron diffraction (CBED) technique is the most suitable approach for this purpose – due to large lattice parameters of the E-phase CBED disks overlapped, which made it impossible to use this approach. Thus, the symmetry of the E-phase was estimated from microdiffraction and selected area electron diffraction patterns using the beam precession technique by Morniroli et al. [4,5]. Since the intensities of the diffracted beams of the precession electron diffraction (PED) patterns are integrated, they are closer to the kinematical intensities [6–8]. Thus, an accurate assessment of the PED patterns provides a possibility of more precisely deriving the extinction conditions and characterizing the space group. Among the possible point groups, corresponding to the orthorhombic system, only *mmm* or 222 can be associated with the 2*mm* symmetry of the zero-order Laue zone (ZOLZ) PED patterns, which is seen in the patterns taken along the [1 0 0], [0 1 0] and [0 0 1] orientations (Fig. 2a–c, respectively). Since the symmetry of the [0 1 1] ZOLZ PED pattern

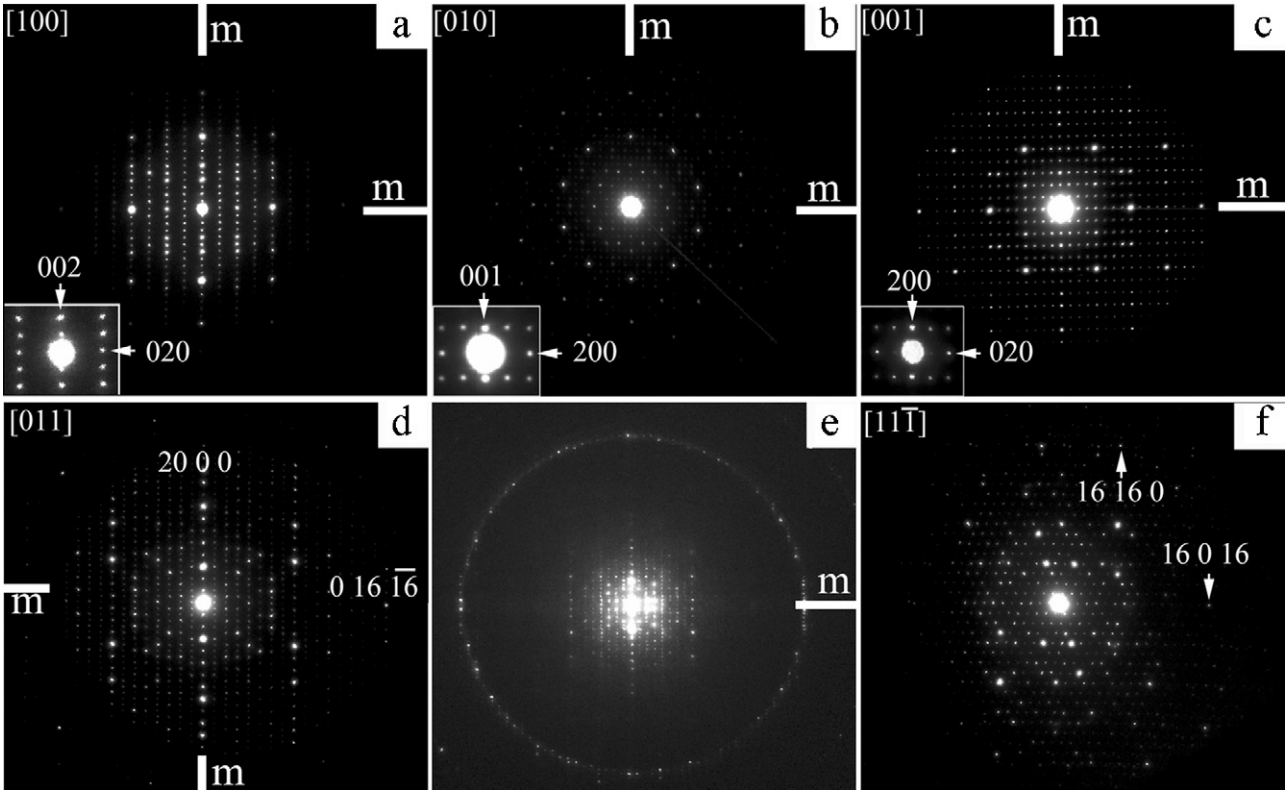

Fig. 2. Electron diffraction patterns taken from the E-phase along: (a) [1 0 0], (b) [0 1 0], (c) [0 0 1] orientations (schematic indexed patterns are shown in the corresponding insets). The mirror planes are labeled by *m*. The precession electron diffraction pattern in (d) and microdiffraction pattern in (e) are taken along the [0 1 1] orientation of the E-phase and the precession electron diffraction in (f) along the [1 1 $\bar{1}$] orientation. The patterns (b), (c), (e) and (f) were obtained with a precession angle of ~2° (34.9 mrad). Reflections with high d_{hkl} value, which appear close to the transmitted beam, have dynamical nature, thus some extra reflections, such as (1 0 1) in Fig. 2f are visible.

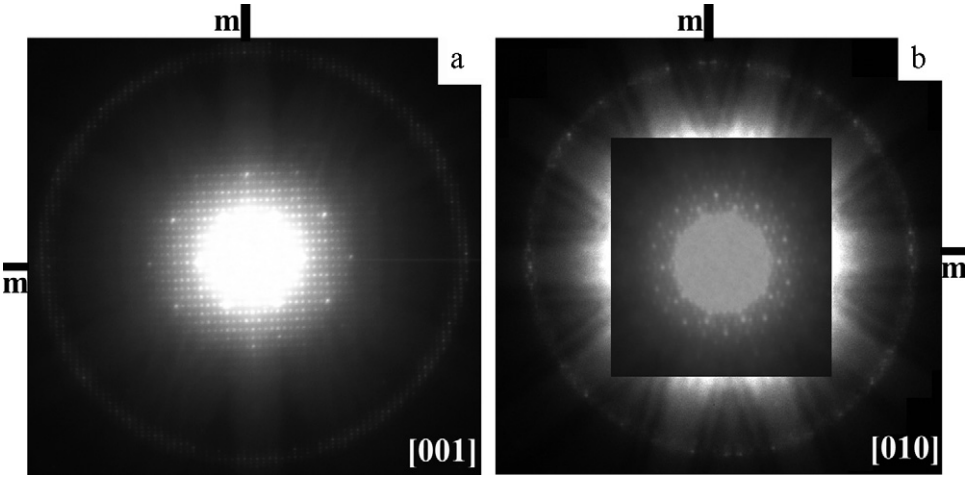

Fig. 3. Electron microdiffraction patterns taken from the E-phase along: (a) [0 0 1] and (b) [0 1 0] orientations. The mirror planes are labeled by *m*. Fig. 3b is a combination of two images taken under the same conditions with different exposure times. This combination allows showing both ZOLZ and FOLZ reflection nets simultaneously.

is *2mm* and that of the [0 1 1] Whole Pattern (WP) is *m* (see Fig. 2d and e, respectively), the correct point group that describes the symmetry of the new $Al_{77}Rh_{15}Ru_8$ phase is *mmm*. In order to check the correctness of the proposed point group, a PED pattern was taken along the $[1\,1\,\bar{1}]$ orientation (see Fig. 2f). Its symmetry can be assessed as 2 and not 1 providing an additional proof of the correctness of the proposed point group.

Full space group symbol can be concluded by combination of the point group with the extinction symbol. In order to estimate reflection conditions and derive extinction symbol – a detailed analysis of the PED patterns taken from the particles of the E-phase was performed. We would like to note that, although most SAD patterns were taken in beam-precession mode, some forbidden reflections still appeared by double diffraction in the PED patterns. Higher precession angle was not always an option on all particles since it leads to doubling of the reflections. An example of the appearance of the forbidden $(0\,k\,0)$-type reflections in the [0 0 1] zone axis pattern is exhibited in Fig. 2c (the inset shows a schematic representation without the forbidden reflections). In order to overcome this obstacle all major zone axis patterns were tilted around the reciprocal rows containing the suspected forbidden reflections (such as reflections of the $(0\,0\,h)$, $(0\,k\,0)$, $(0\,0\,l)$, $(h\,k\,0)$, $(h\,0\,k)$ and $(h\,k\,0)$ type). The forbidden reflections vanished while the intensities of the allowed reflections were almost not affected. As a result, the following reflection conditions were revealed: for the $(h\,0\,0)$ and $(h\,k\,0)$ reflections $h=2n$ and for the $(0\,k\,l)$ and $(0\,k\,0)$ type reflections $k=2n$. According to the International Tables of Crystallography [9], the extinction symbol related to these reflection conditions is $Pb-a$.

An additional way to check the proposed extinction symbol and estimate the space group is to obtain microdiffraction patterns at principal orientations and evaluate their symmetries as well as shifts and periodicity differences among the reflection nets of the zero-order (ZOLZ) and first-order (FOLZ) Laue zones [5]. Microdiffraction patterns taken along the [0 0 1] and [0 1 0] orientations are shown in Fig. 3a and b, respectively. Since these patterns exhibit mirror symmetries parallel to the (1 0 0), (0 1 0) and (0 0 1) planes, the symmetry of these patterns was determined as *2mm* for the whole patterns (WP). This identifies the crystal system as orthorhombic [5], in agreement with the conclusion reached before. Since no shifts were observed between the ZOLZ and FOLZ reflection nets at these orientations, it proved that the Bravais lattice should be of the P-type. Due to the ZOLZ/FOLZ periodicity differences observed in both [0 1 0] and [0 0 1] patterns and no such differences in [1 0 0] WP (not shown in present article), it was concluded that two glide planes exist, namely the glide plane of *b*-type perpendicular to the (1 0 0) plane and the glide plane of the *a*-type parallel to the (0 0 1) plane. This finding supports the proposed $Pb-a$ extinction symbol, derived earlier.

The combination of the *mmm* point group with the $Pb-a$ extinction symbol results in the *Pbma* space group. However, the difference among the *m* and *2mm* symmetries of the relevant ED patterns might be subtle, thus this conclusion should be supported. Both *Pbma* (no. 57) and $Pb2_1a$ (no. 29) space groups possess the same extinction symbol, so they are the only possible variants of the space group that describes the symmetry of the E-phase. The projection symmetries of these two space groups along the principal axes are different. It is possible to determine the projection symmetry of the E-structure analyzing the phases extracted from the Fourier transform of the HRTEM image taken along this axis. This was performed using program CRISP [10]. The *pmg* projection symmetry of the HRTEM image taken along the [0 1 0] orientation (Fig. 4a) was concluded, since it gave a lowest average phase error (phase residual = 17.4°). Evaluation of the projection symmetry of the [0 0 1] HRTEM image (see Fig. 4d) revealed the *pgm* projection symmetry, since it produced the lowest average phase error (phase residual = 14.3°). Thus, the only possible space group which describes the symmetry of the E-phase is *Pbma* (no. 57, setting 5).

Analyzing the structure of the E-phase we noticed that its *a* and *b* lattice parameters are the same as of the known ε-phases, while the *c* lattice parameter is $\sim\tau$ times larger than that of ε_6 (and subsequently $\sim\tau$ times smaller than that of ε_{16}). A structural model of ε_6 was determined in Ref. [11] and of ε_{16} in Ref. [12].

According to the lattice parameters, the new structure might be ε_{10} – naturally closing a "gap" between ε_6 and ε_{16}. However, we cannot include it in the ε-series described in [13,14], since the tiling of the E-structure is different from that of ε–s, as can be seen in the HRTEM images taken from the new phase. This is illustrated in Fig. 4b and c, where the tiling elements typical of the ε-phases, i.e., flattened hexagon and pentagon, are also shown for comparison.

The periodicities of the ε-structures in the *c* direction are combined from the basic short distances $S\approx 0.76$ nm and long distances $L=\tau S\approx 1.23$ nm (see Ref. [13] and references therein). Here *S* is the diameter of the "clusters" building the structure and is the shortest distance between the vertices of the hexagons and pentagons creating the tiling of ε–s, while *L* is the diagonal of the pentagon, so for all ε–s (see Ref. [13]) $a=2\sqrt{(L^2-S^2/4)}=S\sqrt{(4\tau+3)}\approx 2.34$ nm,

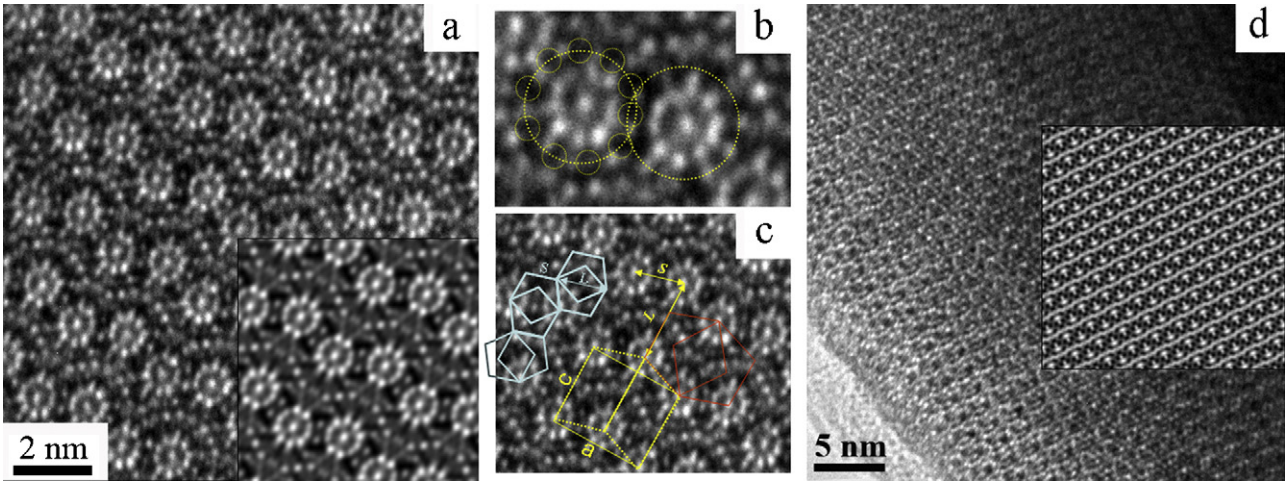

Fig. 4. (a) HRTEM image taken from the Al–Rh–Ru E-phase along the [0 1 0] direction. The image corrected by CRISP is shown in the inset. It corresponds to the optimal defocus and the exact zone axis alignment. Plane group symmetry *pmg* was imposed on the image Fourier components. (b and c) Enlarged portions of the image in (a) and their tiling. The basic "clusters" of the E-phase structure are emphasized in (b). The parallelogram tiling of the image in (c) (dotted yellow line) is constructed from the short (***S***) and long (***L***) elements. The projection of the unit cell with the *a* and *c* lattice parameters is shown by the yellow solid line. For comparison, the hexagonal and pentagonal tiling elements of the ε_6 and ξ phases are shown in blue and the same τ-times larger elements in red. (d) HRTEM image taken from the Al–Rh–Ru E-phase along the [0 0 1] direction. The image corrected by CRISP is shown in the inset. It corresponds to the optimal defocus and the exact zone axis alignment. Plane group symmetry *pgm* was imposed on the image Fourier components. (For interpretation of the references to color in this figure legend, the reader is referred to the web version of the article.)

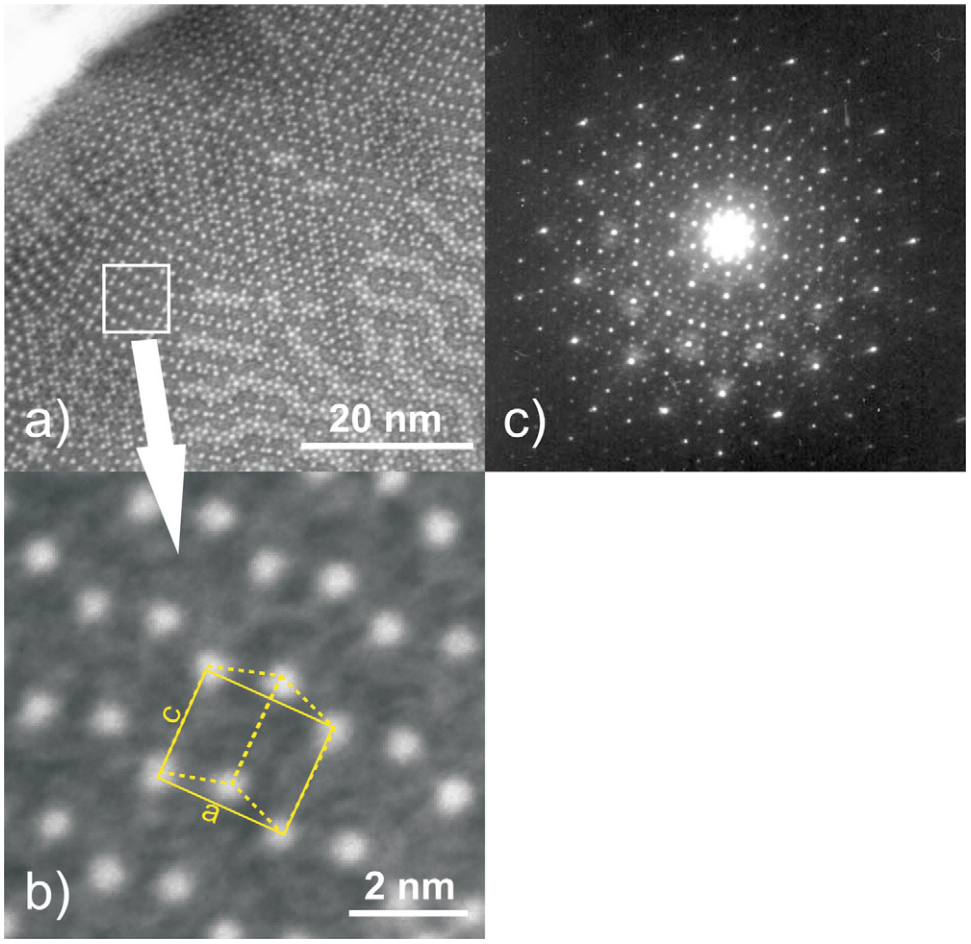

Fig. 5. Lattice image (a and b) of the Al–Pd–Ru E-phase(s) along the [0 1 0] direction and its tiling, and the corresponding electron diffraction pattern (c). In (b) the selected domain can be presented by the same tiling as that in Fig. 4. (For interpretation of the references to color in this figure legend, the reader is referred to the web version of the article.)

while:

- for ε_6: $c = (L) \approx 1.23$ nm;
- for ε_{10}: $c = (L + S) \approx 2.00$ nm (*hypothetic* case);
- for ε_{16}: $c = (2L + S) \approx 3.22$ nm;
- for ε_{22}: $c = (3L + S) \approx 4.45$ nm;
- for ε_{28}: $c = (4L + S) \approx 5.68$ nm.

Two characteristic distances of the E-phase related by τ can be clearly seen: short distances designated $\boldsymbol{S}$ and long designated $\boldsymbol{L}$. They are respectively $\sim\tau$ times larger than the above-mentioned S and L of ε–s (in order to discriminate from S and L they are written in *bold italic*). This implies that the structure of the E-phase is built from the clusters τ-times larger than those of the ε-phases. The distance $\boldsymbol{S} \approx 1.23$ nm corresponds to the diameters of the clusters, and the lattice parameters of the E-phase are: $a = \boldsymbol{S}\sqrt{(4 - 1/\tau^2)} = S\sqrt{(4\tau + 3)} \approx 2.34$ nm and $c = \boldsymbol{L} = \tau\boldsymbol{S} \approx 2.00$ nm.

It is worth noting that apart from the above-mentioned ε-phases, the so-called ξ-phase (*Bmmb*, $a \approx 2.00$, $b \approx 1.62$ and $c \approx 1.45$ nm) was reported. It is constructed from the same flattened hexagons as ε_6 but arranged in parallel (see for example Ref. [15]). Its lattice parameter b is the same as for ε–s, while a is τ times larger than the c lattice parameter of ε_6, and c is τ times smaller than the a lattice parameter of ε_6. The ξ-phase was observed in solidified Al–Pd–Mn alloys but not in those additionally thermally annealed at sufficiently high temperatures [16].

A structure similar to the present E-phase was revealed earlier in the Al–Pd–Ru alloy system, and the corresponding phase was also designated E (in Ref. [17] this phase is mentioned without structural details). Similar to that in Al–Rh–Ru, it is formed close to the high-Ru limit of the ε-region extending, in this case, from binary Al–Pd.

A lattice image of the Al–Pd–Ru E-phase in Fig. 5 shows small domains with different features. All domains have the same periodicity of ~1.6 nm in the direction perpendicular to the pseudo-tenfold plane. They are formed inside the grains of several microns in diameter. In the plane perpendicular to the b-axes the overall symmetry of the diffraction patterns taken from the grains is pseudo-tenfold (Fig. 5c). These different structural variants based on a τ-times larger "cluster" can probably be associated with another family of structures. In Al–Pd–Ru the E-structures were revealed at temperatures lower than those of the high-Ru ε-phases. Close examination revealed a compositional gap of ~1 at.% between the E-range and ε-range at 790 °C, while no visible compositional differences were revealed at 900 °C [17].

4. Conclusions

In conclusion, a new complex intermetallic phase $Al_{77}Rh_{15}Ru_8$ (E-phase) has been identified in the Al–Rh–Ru alloy system. It has an orthorhombic unit cell with lattice parameters $a = 2.34$, $b = 1.62$ and $c = 2.00$ nm; its crystal symmetry can be described by the *Pbma* space group. The [0 1 0] electron diffraction pattern of the E-phase exhibits pseudo-tenfold symmetry, which is also typical of the Al–Pd(Rh)–TM ε-phases. The b lattice parameter of both E and ε–s is also typical of the periodicity of the decagonal D_4 structure observed in binary and ternary Al–TM alloys. Despite a great similarity between E and the structures of the known ε-family, the relation among them needs further specification.

Acknowledgements

Technical assistance by V. Ezersky, V. Lenzen and C. Thomas is gratefully acknowledged. We also thank M.G. Li for valuable discussions. D.K. thanks Forschungszentrum Jülich for financial support and hospitality.

References

[1] B. Grushko, T.Ya. Velikanova, Calphad 31 (2007) 217.
[2] B. Grushko, J. Gwóźdź, M. Yurechko, J. Alloys Compd. 305 (2000) 219.
[3] S. Mi, S. Balanetskyy, B. Grushko, Intermetallics 11 (2003) 643.
[4] J.P. Morniroli, A. Redjaimia, S. Nicolopoulos, Ultramicroscopy 107 (2007) 514.
[5] J.P. Morniroli, J.W. Steeds, Ultramicroscopy 45 (1992) 219.
[6] R. Vincent, P.A. Midgley, Ultramicroscopy 53 (1994) 271.
[7] K. Gjonnes, Ultramicroscopy 69 (1997) 1.
[8] P. Oleynikov, S. Hovmöller, X.D. Zou, Ultramicroscopy 107 (2007) 523.
[9] T. Hahn (Ed.), International Tables for Crystallography, vol. A, Kluwer Acad. Publ., Dordrecht/Boston/London, 1992.
[10] S. Hovmöller, Ultramicroscopy 40 (1992) 121.
[11] M. Boudard, H. Klein, M. de Boissieu, M. Audier, H. Vincent, Philos. Mag. A 74 (1996) 939.
[12] M.G. Li, J.L. Sun, P. Oleynikov, S. Hovmöller, X.D. Zou, B. Grushko, Acta Crystallogr. B 66 (2010) 17.
[13] S. Balanetskyy, B. Grushko, T.Ya. Velikanova, Z. Kristallogr. 219 (2004) 548.
[14] M. Yurechko, A. Fattah, T. Velikanova, B. Grushko, J. Alloys Compd. 329 (2001) 173.
[15] H. Klein, M. Audier, M. Boudard, M. de Boissieu, L. Beraha, M. Duneau, Philos. Mag. A 73 (1996) 309.
[16] S. Balanetskyy, G. Meisterernst, M. Heggen, M. Feuerbacher, Intermetallics 16 (2008) 71.
[17] D. Pavlyuchkov, B. Grushko, T.Ya. Velikanova, J. Alloys Compd. 469 (2009) 146.